Heat Release Rate of Fires under a Ceiling Calculated from Measurements in the Ceiling Layer

Zhou X.

FM Global, Research Division 1151 Boston-Providence Turnpike, Norwood MA, USA
xiangyang.zhou@fmglobal.com

ABSTRACT

The heat release rate (HRR) is often the most important quantity to characterize fire growth and suppression. However, it is still a challenge to obtain a time-resolved HRR for a fire experiment conducted under a ceiling. This work proposes a new method to calculate the convective and chemical HRRs for a fire under a ceiling. The instantaneous measurements of gas temperature, velocity and species concentration in the ceiling layer are used to calculate the HRRs. To verify the proposed method, two heptane pan fire tests are conducted under a ceiling and the chemical HRR is calculated from the fuel mass loss data. The results show that the proposed method can provide a time-resolved chemical HRR that is comparable to that obtained from the fuel mass loss rate. The fraction of convective HRR to chemical HRR also agrees well with the test data obtained under a calorimeter.

KEYWORDS: Ceiling jet, fire, heat release rate.

INTRODUCTION

The time-resolved HRR can usually be measured directly under a fire calorimeter (or fire product collector). Figure 1 shows a sketch of a fire under a 20-MW calorimeter. The gaseous combustion products are drawn directly into the hood, where gas species concentrations, gas velocity and gas temperature are measured downstream in the exhaust duct. Based on these measurements, the chemical HRRs ($\dot{Q}_{chem,O_2}$ or $\dot{Q}_{chem,CO_2CO}$) can be calculated based on either oxygen consumption or CO_2/CO generation [1] as

$$\dot{Q}_{chem,O_2} = \dot{m}_{flow} \frac{M_{O_2}}{M_{mix}} \Delta h_{O_2} \left(x_{O_2,\infty} - x_{O_2} \right). \quad (1)$$

$$\dot{Q}_{chem,CO_2CO} = \dot{m}_{flow} \left[\frac{M_{CO_2}}{M_{mix}} \Delta h_{CO_2} \left(x_{CO_2} - x_{CO_2,\infty} \right) + \frac{M_{CO}}{M_{mix}} \Delta h_{CO} \left(x_{CO} - x_{CO,\infty} \right) \right]. \quad (2)$$

The quantity $\dot{m}_{flow}$ is the total mass flow rate of gas mixture in the exhaust duct, and M_{O2}, M_{CO2}, M_{CO} and M_{mix} are the molecular weights of O_2, CO_2, CO and gas mixture in the exhaust duct, respectively. The molecular weight of the gas mixture is approximated as that of air. The quantities Δh_{O_2}, Δh_{CO_2} and Δh_{CO} are the heat production associated with oxygen consumption and CO_2 and CO generation, which depend on fuel components and chemistry [1]. The quantities x_{O_2}, x_{CO_2} and x_{CO} are the measured volumetric fractions of each gas species.

The convective HRR ($\dot{Q}_{conv}$) is calculated as

$$\dot{Q}_{conv} = \dot{m}_{flow} c_p (T - T_0), \quad (3)$$

where T_0 is ambient air temperature and c_p is the specific heat of gases. Although there are time delay and signal smearing due to gas transport and sampling, adjustment for these effects can be

Proceedings of the Ninth International Seminar on Fire and Explosion Hazards (ISFEH9), pp.608-618
Edited by Snegirev A., Liu N.A., Tamanini F., Bradley D., Molkov V., and Chaumeix N.
Published by St. Petersburg Polytechnic University Press
ISBN: 978-5-7422-6496-5 DOI: 10.18720/spbpu/2/k19-11

made so that the time-resolved accuracy of both chemical and convective HRRs is acceptable for the calorimeter measurements.

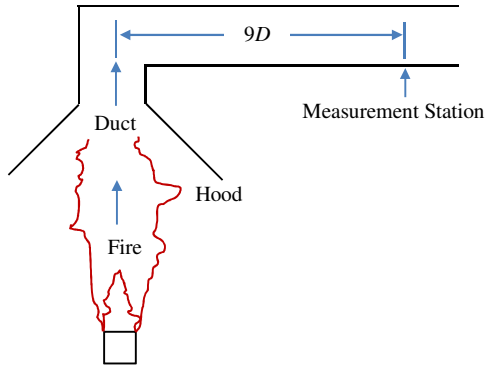

Fig. 1. Illustration of a fire under the 20-MW calorimeter (D – duct diameter).

In contrast, for a fire experiment conducted under a ceiling, it is a challenge to obtain the time-resolved HRR. Figure 2 illustrates a fire under a movable ceiling in a large testing laboratory, which shows the ceiling jet, the combustion products above the ceiling, and the exhaust direction at the lab ceiling level. Because of the large volume of plenum space above the ceiling, the combustion products generated at different times tend to accumulate and mix in that space. Therefore, the gas mixture that is drawn into the exhaust ducts is different from what the fire is generating at a given time and the measured gas concentrations are not time-resolved. Because of this mixing in the plenum space above the ceiling, a time-resolved HRR is not possible through direct measurements of the exhaust gases in the duct at the lab ceiling.

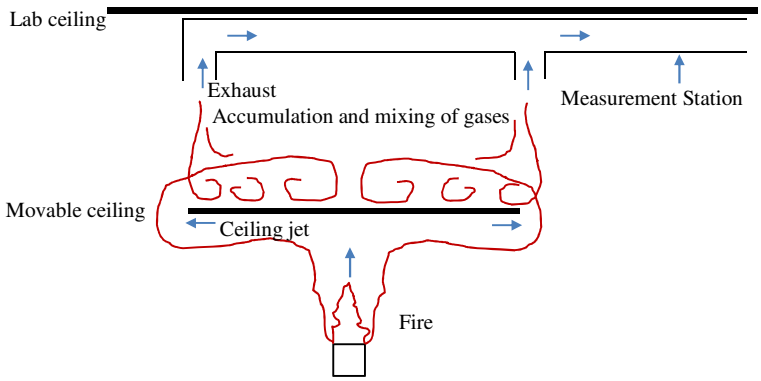

Fig. 2. Illustrations of a fire under a ceiling with a ceiling jet and combustion products above the ceiling.

To account for accumulation and mixing of the combustion products within the large volume of space above the movable ceiling, a method has been proposed to correct the species concentration data by a time parameter [2]. Data from a limited number of tests indicated that a simple first-order correction is still inadequate. Another method, developed to estimate the time-resolved HRR by using the flame volume [3], is based on the assumption that the chemical HRR per unit flame volume is relatively invariant, as long as the combustion is controlled by diffusion in buoyant fires under well-ventilated conditions. This method can be used for certain fire scenarios with simple geometries where the flame volume can be estimated with confidence.

Estimates of the convective HRR obtained from measurements of gas temperature near the ceiling have already been reported [4]. Following the above effort, this work will pursue a new approach where the instantaneous measurements of gas temperature, velocity and species concentrations in the ceiling jet are used to calculate both convective and chemical HRRs. To verify the proposed method, two heptane pan fire tests are conducted under the movable ceiling. The chemical HRR of the heptane pan fire is calculated from the fuel mass loss rate based on the load-cell data. This direct measurement is then used to verify the calculation obtained from the proposed method.

EXPERIMENTAL SETUP

The heptane pan fire tests were conducted under the North Movable Ceiling (NMC) in the Large Burn Lab (LBL) located at the FM Global Research Campus. The NMC measures 24.4 m × 24.4 m in size and is adjustable for heights above the floor ranging from 3.1 m to 18.3 m. The exhaust ductwork of the air emission control system for the movable ceiling consists of four extraction points, located at the lab ceiling (20.4-m high), that merge into a single duct with a cross sectional area of 6.1 m^2. The air exhaust rate from the lab space was 118±4 kg/s.

Figure 3 shows the pan fire test setup in elevation view and a fire image captured in the test. The pan fires were established on a 109 cm diameter, 15 cm high steel pan filled with 38 liters of heptane (4.1 cm deep) on a layer of 7.6 cm deep water. The fuel pan was placed under the ceiling center and 94 cm above the floor on a stand. A load cell of 181±0.002 kg capacity, thermally insulated from the steel pan, was used to measure the mass loss rate of the heptane fuel. The flame height of the fire shown in Fig. 3 was about 4 m above the pan.

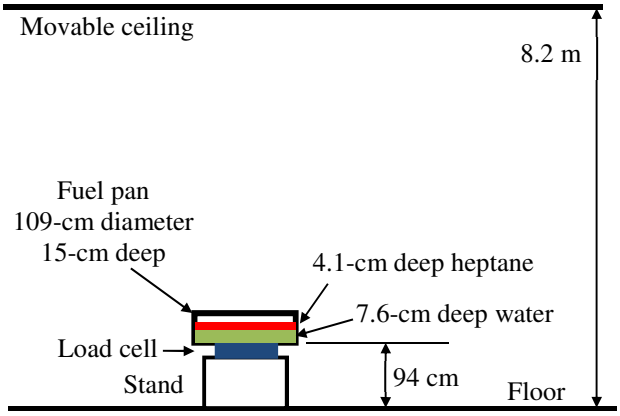

Fig. 3. Elevation view of the heptane pan fire under a movable ceiling and a fire image captured in the test.

The ceiling height was 8.2 m above the floor providing a 7.1 m clearance above the fuel pan. There were 125 thermocouples (TCs) installed 0.15 m below the ceiling to measure the gas temperatures. Figure 4 shows the locations of the 125 TCs. The TC labeled #113 was at the ceiling center. Figure 4 also shows the locations of the 12 bi-directional velocity probes (OD 22 mm) with corresponding TCs that were installed along four directions (N, E, S and W) and at three radial distances from the ceiling center. In the region near the ceiling center, the two radial distances of 2.1 and 4.0 m were the same for all four directions. Toward the outer edge of the ceiling, the velocity probes were installed at a radial distance of 10.7 m in the W-E direction and 10.4 m in the N-S direction. The velocity probes were located 0.11 m below the ceiling.

To measure the vertical temperature distribution within the ceiling layer flow, four TC trees were installed along four directions (N, E, S and W) at a 4.0 m radial distance from the ceiling center. The locations of the four TC trees are illustrated in Fig. 4. Each TC tree is 1.22 m in length and includes four vertically-spaced TCs (K-type, 28-gauge bare bead) as shown in Fig. 5. Because the TC trees were located near a bi-directional velocity probe, the four TCs of the TC tree and the TC of the velocity probe were combined to describe the vertical temperature distribution. Four gas sampling probes (see Fig. 5) were installed at the same four locations as the TC trees and facing the fire to extract ceiling gases for species concentration measurements. Each gas sampling probe is 6.3 mm in diameter and 11 cm below the ceiling. Because only one gas analyzer was available in the LBL, the four gas sampling lines were merged into one and then connected to the Gas Sampling Cabinet. The locations of the four gas sampling probes are also illustrated in Fig. 4. Because of radiative heating from the pan fire, the gas temperature obtained from the bare-bead TC measurement was corrected using the method developed in Ref. [5]. Two heptane pan fire tests were conducted under the same test conditions.

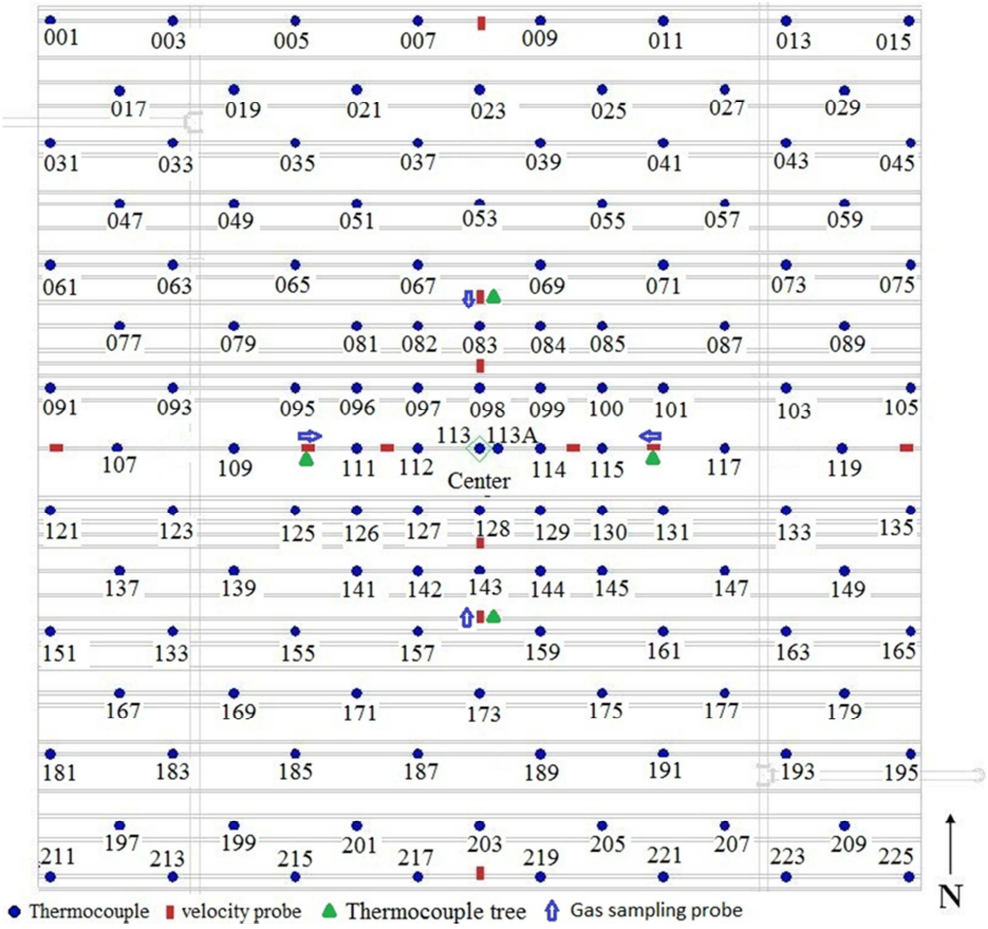

Fig. 4. Illustration of the locations of 125 ceiling TCs, 12 bi-directional gas velocity probes, four gas sampling probes and four TC trees.

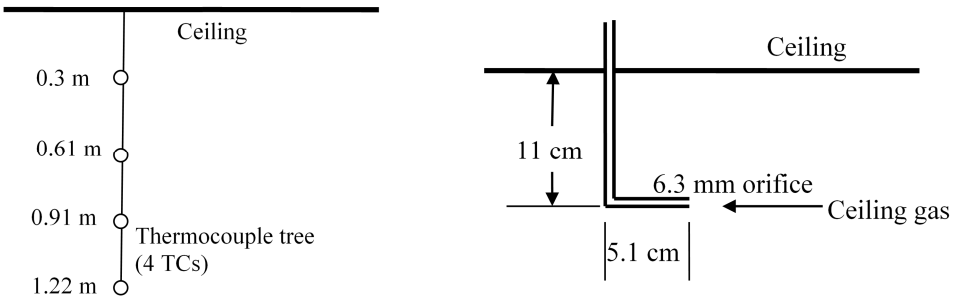

Fig. 5. Sketch of a TC tree with four TCs and a gas sampling probe (with TC) installed under the ceiling.

HEAT RELEASE RATE (HRR) CALCULATION

The method for the time-resolved HRR calculation is developed based on the assumption that the ceiling jet flow under the ceiling is horizontal and outward from the ceiling center. Figure 6 shows a sketch of the elevation view and top view of the ceiling jet flow for a fire under a horizontal ceiling. The dashed lines in Fig. 6 define the control volume enclosed by a cylinder of radius (r) around the ceiling center. The instruments are assumed to be placed along the cylinder surface at different heights to measure the gas velocity, temperature and species concentration of the outward gases through the cylindrical boundary. These should be made at a sufficient distance from the ceiling center so that an outward flow is still observed even if the fire axis moves away from the ceiling center. In a fire test where ceiling sprinklers have activated, the disruption caused by the downward flow of the sprinkler spray will require that the measurements be made at a sufficiently large radius to avoid the resulting near-field effects.

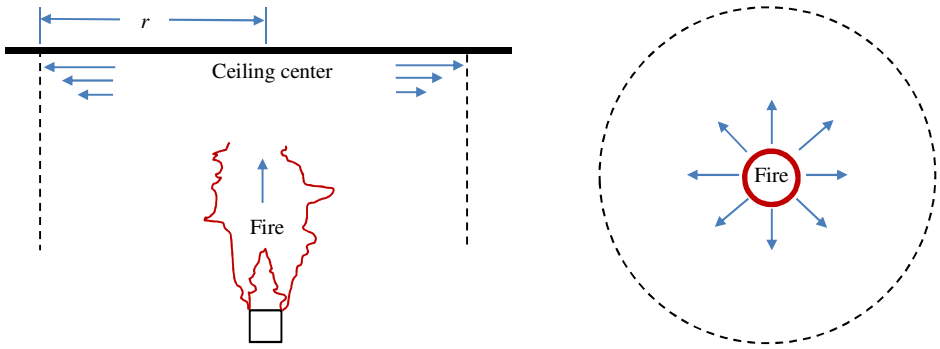

Fig. 6. Sketch of elevation view and top view of the ceiling jet flow of a fire under a horizontal ceiling.

Based on the above assumption of axisymmetric outflow through the cylindrical boundary of radius r, the total instantaneous mass flow rate of the ceiling jet flow is given by

$$\dot{m}_c(r) = 2\pi r \int_0^{z_c} \rho(z,r)u(z,r)dz, \tag{4}$$

where z is the height below the ceiling, z_c is a height chosen to include the whole ceiling jet flow, $\rho(z,r)$ is the density of the gas, and $u(z,r)$ is the horizontal velocity component of the gas under the ceiling. The ceiling gas density is obtained from the ideal gas law as

$$\rho(z,r) = pM/RT(z,r), \tag{5}$$

where p is ambient pressure, M is the gas molecular weight, R is the ideal gas constant, and $T(z, r)$ is the gas temperature. The ceiling layer temperature distribution along the height can be described by an empirical correlation developed in previous work [6] as

$$T(z,r) - T_0 = \Delta T(z,r) = \Delta T_m(r) exp\left[-\left(\frac{Z-0.102}{\delta_T}\right)^2\right], \quad (6)$$

where T_0 is the ambient gas temperature, $\Delta T(z,r)$ is the temperature rise, $\Delta T_m(r)$ is the maximum temperature rise in the ceiling layer at the radius r, δ_T is the thermal depth of the ceiling layer defined at the location where $\Delta T(z,r) = \Delta T_m(r)/e$, and e is the base of the natural logarithm. The temperature profile $T(z,r)$ was measured in this work by five TCs installed at the same radius (r) and different heights (z) (cf. Fig. 5). Based on these measurements, the two parameters ΔT_m and δ_T can be obtained by curve fitting. The integral limit z_c was assumed as $3\delta_T + 0.102$.

The radial outward velocity in the ceiling layer is described by a similar empirical correlation [6] as

$$u(z,r) = u_m(r) exp\left[-\left(\frac{Z-0.102}{\delta_u}\right)^2\right], \quad (7)$$

where $u_m(r)$ is the maximum radial velocity in the ceiling layer at radius r, and δ_u is the depth of the velocity profile in the ceiling layer. The value of δ_u is correlated to δ_T [6] as $\delta_u = 0.67\delta_T$.

Similar to the gas temperature, the species volume fraction (x_i) distribution in the ceiling layer is assumed to have the same Gaussian profile as

$$x_i(z,r) - x_{i,0} = \Delta x_{i,m}(r) exp\left[-\left(\frac{Z-0.102}{\delta_x}\right)^2\right], \quad (8)$$

where $\Delta x_{i,m}$ is the maximum species volume fraction difference in the layer and δ_x is the depth of the species profile. If there are enough instruments to measure species concentration, the profile $x_i(z,r)$ in Eq. (8) can be determined by obtaining $\Delta x_{i,m}$ and δ_x. However, since only one gas analyzer was available in this work, a single value of x_i was measured at a height (z = 0.11 m) below the ceiling. In addition, this measurement represented an average from the four azimuthal locations. In order to generate the species profile $x_i(z,r)$, two approximations were made in this work.

The first approximation is to assume $\delta_x = \delta_T$, although δ_x and δ_T may be different since, outside of the flame region, x_i is a conserved variable while T is not conserved due to heat transfer. The value of δ_x is also assumed to change with δ_T at different times and locations. Because only one spatially-averaged value of x_i is available, the second approximation is to assume that the species concentrations at the same height (and radius) but different azimuthal locations are the same. After obtaining δ_x and x_i at z = 0.11 m, Eq. (8) was used to calculate the value of $\Delta x_{i,m}$. The profile of $x_i(z,r)$ in the ceiling layer was then determined from $\Delta x_{i,m}$, δ_x and Eq. (8). Because the spatially-averaged value of x_i is time-resolved, the total chemical HRR can also be time-resolved and can be calculated from CO/CO_2 generation or oxygen consumption as

$$\dot{Q}_{chem,CO_2CO}(r) = 2\pi r \frac{M_{CO_2}}{M_{mix}} \Delta h_{CO_2} \int_0^{z_c} \rho(z,r)u(z,r)\left[x_{CO_2}(z,r) - x_{CO_2,\infty}\right]dz + 2\pi r \frac{M_{CO}}{M_{mix}} \Delta h_{CO} \int_0^{z_c} \rho(z,r)u(z,r)\left[x_{CO}(z,r) - x_{CO,\infty}\right]dz, \quad (9)$$

$$\dot{Q}_{chem,O_2}(r) = 2\pi r \frac{M_{O_2}}{M_{mix}} \Delta h_{O_2} \int_0^{z_c} \rho(z,r)u(z,r)\left[x_{O_2,\infty} - x_{O_2}(z,r)\right]dz. \quad (10)$$

The convective HRR is calculated as

$$\dot{Q}_{conv}(r) = 2\pi r \int_0^{z_c} \rho(z,r)u(z,r)c_p[T(z,r) - T_0]dz. \quad (11)$$

Based on the method described above, a computer code was developed to post-process the test data and to calculate the convective and chemical HRRs. The fire center in the ceiling layer is determined as the location of the maximum temperature measured by the 125 TCs installed under the ceiling. The above integrations at the radius *r* are then calculated separately in four sectors along four directions (N, E, S and W) where the measurements are made. If the fire center in the ceiling layer moves away from the ceiling center, the integration can be calculated in four sections with different sizes. Generally, the integration will be less sensitive to this movement if the moving distance is relatively short. Because of the transport time from the gas sampling probe to the gas analyzers, the species concentration measurements are delayed as compared to the velocity and temperature measurements. This delay time can be determined by aligning the time evolution profiles of the pertinent measurements. Another delay time is the transport time from the fire source to the measuring location (the dashed circle shown in Fig. 6). This delay time depends on the gas velocity in the fire plume and the ceiling layer and will be a function of the HRR.

RESULTS AND DISCUSSION

Figure 7 shows the load-cell data recorded in Test #1 (one of the two heptane pan fire tests) and the corresponding chemical HRR calculated from the fuel mass loss rate. The net heat of complete combustion per unit mass of heptane is 44.6 kJ/g, and the combustion efficiency is $\eta = 0.92$ [1]. Therefore, the expected chemical HRR of the heptane pool fire was calculated from the heptane mass loss rate based on the load-cell data. The time $t = 0$ s denotes ignition. After an initial growth period (< 100 s), the data show that heptane was consumed at an approximately constant rate. The total burning time was about 10 minutes. In the time period from 200 s to 500 s, the average HRR calculated from fuel mass loss rate is 1880 kW.

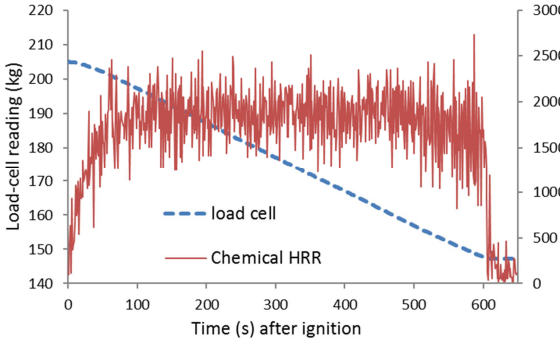

Fig. 7. The load-cell data recorded in Test #1 and the chemical HRR calculated from fuel mass loss rate.

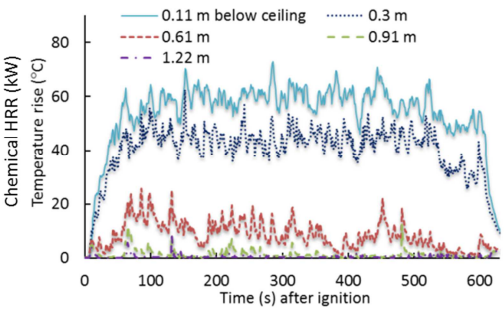

Fig. 8. Gas temperature rise measured by five TCs installed at different heights and the same radius (4.0 m) east of the ceiling center for Test #1.

The method developed in this work was used to calculate the chemical HRR. For Test #1, Fig. 8 shows five temperature profiles measured by a TC tree with five TCs installed at different heights but at the same radius (4.0 m) east of the ceiling center. The figure shows that the gas temperature rise decreased with the distance from the ceiling. After 100 s, the ceiling gas temperatures reached their respective maxima, remained roughly constant, and then decreased when the fuel burned out. There are similar ceiling temperature profiles measured at the other TC trees.

Figure 9 shows the time evolutions of ΔT_m and δ_T determined based on the empirical ceiling profiles and the temperatures shown in Fig. 8. During the initial period before significant temperature rise, there were small temperature differences between the five TCs. Therefore, the initial thermal depth (δ_T) is uncertain and is not presented in Fig. 9. When the ceiling gas temperature ΔT_m became sufficiently large, the thermal depth settled at about 0.4 m. Similar ΔT_m and δ_T profiles were also obtained at the south, west and north locations. As an example, for ΔT_m = 61.8 °C and δ_T = 0.38 m at time t = 250 s, Fig. 10 shows five temperature measurements and the empirical profile from Eq. (6) as $\Delta T(z) = 61.8exp\left[-\left(\frac{Z-0.102}{0.38}\right)^2\right]$. The plot shows that the five temperature measurements are well described by the profile.

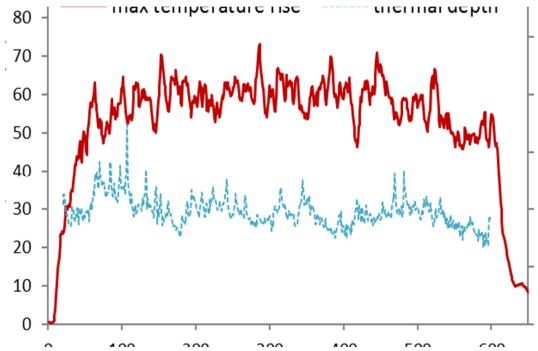

Fig. 9. Values of ΔT_m and δ_T calculated using the temperature profiles measured at 4.0 m east of the ceiling center for Test #1.

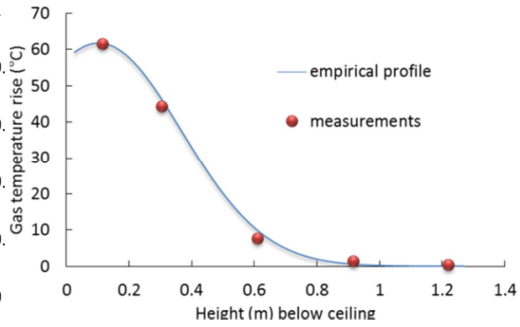

Fig. 10. An empirical temperature profile and five temperatures measured at t = 250 s and 4.0 m east of the ceiling center for Test #1.

Figure 11 shows the time evolutions of the ceiling layer velocity measured at 4.0 m east of the ceiling center. The velocity profile is similar to the temperature profiles shown in Fig. 9. The CO_2 volume fraction obtained from the gas sampling probe is also presented in Fig. 11. Because CO_2 was generated by fuel burning, the volume fraction profile increased with time and then reached an approximately constant value. Similar to the empirical profile shown in Fig. 10, the profiles for velocity and species volume fraction can also be determined using Eqs. (7) and (8) from the one-point measurements illustrated in Fig. 11. It should be noted that the species concentration measurements were delayed as compared to the velocity measurements because of the transport time from the gas sampling probe to the gas analyzers. Relative to the temperature and velocity data, this delay time was about 40 s.

After obtaining the above results, the method developed in this work was used to calculate the chemical and convective HRRs, with the former shifted to account for transport times. The result for Test #1 is shown in Fig. 12. For comparison, the chemical HRRs (load cell) calculated from the fuel mass loss rate and that (duct) from the measurements made in the exhaust duct above the ceiling are also presented in the figure. The HRR data were smoothed by removing some large fluctuations. Figure 12 shows that the chemical HRRs calculated from the present method, on average, agree well with those calculated from the fuel mass loss rate; however, the HRRs from the duct measurements are delayed and reduced in growth rate due to gas mixing in the volume above the ceiling.

In the initial fire growth period (0 ~ 65 s), Fig. 12 shows that the HRRs of the present method align well with those calculated from the load cell. However, because of gas transport time from the fire source to the measurement station at the ceiling, the HRR data of the present method are about 8 s delayed in comparison to those of the load cell. Based on the slope of the HRR profile in the initial

fire growth period, the average HRR growth rate obtained from the load cell is 22.7 kW/s and 21.2 kW/s for the present method. The relative difference is 7%, which means that the proposed method can provide a time-resolved chemical HRR.

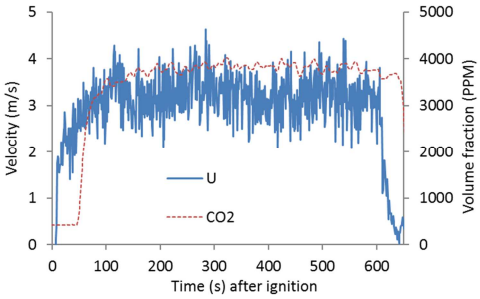

Fig. 11. The ceiling layer velocity measured 4.0 m east of the ceiling center and the CO_2 volume fraction measured from the gas sampling probe for Test #1.

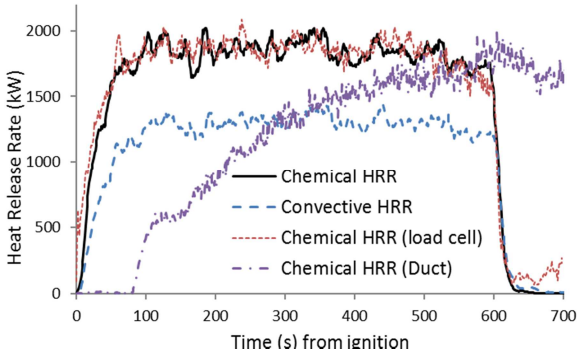

Fig. 12. Convective and chemical HRRs calculated by the present method and the chemical HRR calculated from the fuel mass loss rate and the measurements in the exhaust duct for Test #1.

Roughly, the pan fire reached a steady burning rate after 100 s. In the period from 200 s to 500 s, the average chemical HRR calculated from the present method is 1860 kW, which is very close (1% lower) to the average HRR of 1880 kW calculated from the fuel mass loss rate. It is also noted from Fig. 12 that the HRR from the duct measurements took a long time (~500 s) to reach steady state due to the gas smearing effect above the ceiling. After the fuel burned out at 600 s, both the chemical HRR of the present method and that of the load cell decreased sharply at the same rate. The load cell data remained above zero, due to evaporation of the 7.6 cm deep layer of water in the pan. Data were not collected for a sufficient time following fuel burnout for the duct HRR to return to zero.

Using the HRR profiles shown in Fig. 12, the total heat release can be calculated as the integral of the HRR over the burning time interval. The total heat release was then calculated to be 1070 MJ for the present method, which is 1% lower than the total heat release of 1080 MJ calculated from the fuel mass loss of the 38 liters of heptane.

Figure 12 also shows the convective HRR calculated using the present method. In the same time from 200 s to 500 s, the average convective HRR of the present method is 1320 kW. The fraction of convective HRR to chemical HRR is 71%. The convective HRR cannot be calculated directly from the fuel mass loss rate. Previous tests have shown that the fraction of convective HRR to chemical HRR is in the range of 65% - 75% for heptane fires conducted with different pan sizes [7], which indicates that the convective HRR obtained by the present method is reasonable.

One more comparison is shown in Fig. 13 for the other heptane pool fire test (Test #2). Figure 13 shows the chemical and convective HRRs calculated by the present method, and the chemical HRRs (load cell) calculated from the fuel mass loss rate. The figure shows that the chemical HRRs of the two methods are similar in the growth, steady and decay periods. However, the chemical HRR of the present method is a little higher than that of the load cell. In the same period from 100 s to 500 s, the average chemical HRR of the present method is 2200 kW, which is 10% higher than the average HRR of 2000 kW calculated from the fuel mass loss rate. The total heat release was calculated to be 1180 MJ for the present method, which is 9% higher than the total heat of 1080 MJ released from

the 38 liters of heptane. In the period of 100 – 500 s, the fraction of convective HRR (1540 kW) to chemical HRR (2200 kW) is 70%, which is close to the fraction obtained for Test #1.

The above comparisons show that the present method can determine the chemical HRR of the pan fire tests with an accuracy of about 10%. The uncertainty may come from the test measurements and the empirical correlations used in the present method. It is observed that the difference between the first and the second test comes from the calculation of the total mass flow rate in the ceiling layer. Using Eq. (4), the average mass flow rate was calculated to be 29 kg/s for Test #1 and 32 kg/s for Test #2. The relative difference is about 9%. The difference may come from the gas velocity and temperature calculation estimated from the one-point measurement in the ceiling layer. Test #2 had a higher mass flow rate, resulting in a calculated chemical HRR 10% higher than the value obtained from the fuel mass loss rate.

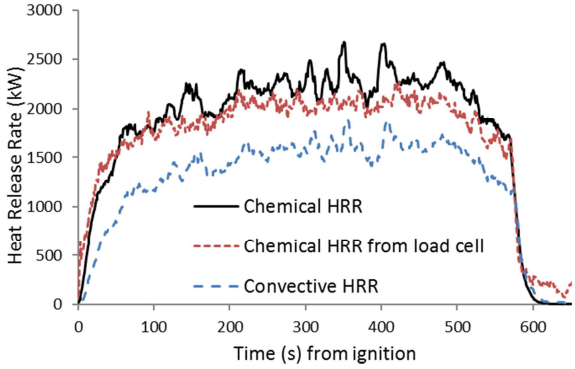

Fig. 13. Convective and chemical HRRs calculated by the present method and the chemical HRR calculated from the fuel mass loss rate for Test #2.

This method has also been used to estimate the HRRs for rack-storage fires under a ceiling and will be reported in another paper. If the assumption for the ceiling jet shown in Fig. 6 is still applicable, generally, this method can provide a near time-resolved HRR that is comparable to that obtained from a similar fuel configuration measured under a calorimeter. For a fire suppression test with downward spray injection, the strong plume-spray interaction can change the ceiling jet. The empirical correlations used for gas temperature, velocity and species concentrations in the ceiling layer need further validation. The measurements of the bare-bead thermocouples and the bi-directional velocity probes may also be affected by the impingement of water droplets. Therefore, this method should be further evaluated with well characterized fire sources under water application to estimate the error and the applicability.

SUMMARY AND CONCLUSIONS

A new method is proposed in this work to calculate the convective and chemical HRRs for a fire conducted under a ceiling. Instantaneous measurements of gas temperature, velocity and species concentration in the ceiling layer have been used to calculate the HRRs. To verify the proposed method, two heptane pan fires were conducted under the ceiling and the chemical HRR was calculated from the heptane mass loss rate based on the load-cell data. In the period for fire growth and fuel burn out, the results show that the proposed method can provide a time-resolved chemical HRR that is comparable to that obtained from the fuel mass loss rate. The fraction of convective HRR to chemical HRR also agrees well with test data obtained under a calorimeter.

There are limits to the range of applicability of the measurement approach introduced here. Barring the introduction of additional gas analysis instrumentation, the current method is based on the assumption of axisymmetric ceiling flow. Also, a well-established outflow at the measurement radius is needed, a requirement which may not be easily satisfied in the case of sprinklered fire tests if measurements are made too close to the fire axis. Increased distance, however, brings about longer travel times and the possible need to correct for them. In conclusion, for ceiling sprinkler-based fire protection tests, this method should be further evaluated with well characterized fire sources in the future.

ACKNOWLEDGMENT

The author would like to thank the FM Global Research Campus staff for conducting the pan fire tests. The valuable suggestions and discussions with Dr. Franco Tamanini, Dr. Hong-Zeng Yu, Dr. Yibing Xin, Dr. Prateep Chatterjee and Dr. Christopher Wieczorek are also greatly appreciated.

REFERENCES

[1] A. Tewarson, Generation of Heat and Chemical Compounds in Fires, Sec. 3, Chap. 4, SFPE Handbook of Fire Protection Engineering, 3rd edition, 2002.

[2] J.S. Newman, C. Wieczorek, J.M.A. Troup, Application of Building-scale Calorimetry, Fire Safety Science–Proceedings of the Eighth International Symposium, pp. 1425-1434, 2005.

[3] Y. Xin, Estimation of Chemical Heat Release Rate in Rack Storage Fires based on Flame Volume, Fire Saf. J. 63 (2014) 29-36.

[4] F. Tamanini, Heat Release Rate and Sprinkler Response Characterization in Large-Scale Fires, Proc. of the Sixth International Seminar on Fire and Explosion Hazards, Edited by D. Bradley, G. Makhviladze and V. Molkov, 2011, pp. 330-341.

[5] W.M. Pitts, E. Braun, E., R.D. Peacock, H.E. Mitler, E.L. Hohnsson, P.A. Reneke and L.G. Blevins, Temperature Uncertainties for Bare-Bead and Aspirated Thermocouple Measurements in Fire Environments, In: Thermal Measurements: The Foundation of Fire Standards, ASTM STP 1427, L.A. Gritzo and N.J. Alvares, Eds., ASTM International, West Conshohocken, PA, 2002.

[6] H.-C. Kung, H.-Z. You, and R.D. Spaulding, Ceiling Flows of Growing Rack Storage Fires, Proc. Combust. Inst. 21 (1986) 121–128.

[7] B.D. Ditch, J.L. de Ris, T.K. Blanchat, M. Chaos, R. G. Bill Jr and S. B. Dorofeev, Pool Fire – An Empirical Correlation, Combust. Flame 160 (2013) 2964-2974.